

PLIF VISUALIZATION AND QUANTITATIVE MIXING MEASUREMENTS OF A SUPERSONIC INJECTION NOZZLE

Carrie A. Noren et al.

16 October 2006

Technical Paper

APPROVED FOR PUBLIC RELEASE; DISTRIBUTION IS UNLIMITED.

**This work is declared a work of the U.S. Government and is not
subject to copyright protection in the United States.**



**AIR FORCE RESEARCH LABORATORY
Directed Energy Directorate
3550 Aberdeen Ave SE
AIR FORCE MATERIEL COMMAND
KIRTLAND AIR FORCE BASE, NM 87117-5776**

REPORT DOCUMENTATION PAGE				Form Approved OMB No. 0704-0188	
Public reporting burden for this collection of information is estimated to average 1 hour per response, including the time for reviewing instructions, searching existing data sources, gathering and maintaining the data needed, and completing and reviewing this collection of information. Send comments regarding this burden estimate or any other aspect of this collection of information, including suggestions for reducing this burden to Department of Defense, Washington Headquarters Services, Directorate for Information Operations and Reports (0704-0188), 1215 Jefferson Davis Highway, Suite 1204, Arlington, VA 22202-4302. Respondents should be aware that notwithstanding any other provision of law, no person shall be subject to any penalty for failing to comply with a collection of information if it does not display a currently valid OMB control number. PLEASE DO NOT RETURN YOUR FORM TO THE ABOVE ADDRESS.					
1. REPORT DATE (DD-MM-YYYY) 16-10-2006		2. REPORT TYPE Technical Paper		3. DATES COVERED (From - To) 01-10-2003 - 01-06-2006	
PLIF VISUALIZATION AND QUANTITATIVE MIXING MEASUREMENTS OF A SUPERSONIC INJECTION NOZZLE (POSTPRINT)				5a. CONTRACT NUMBER In-House (DF299896)	
				5b. GRANT NUMBER	
				5c. PROGRAM ELEMENT NUMBER	
6. AUTHOR(S) Carrie A. Noren*, C. Randall Truman*, Peter V. Vorobieff*, Timothy J. Madden, Gordon D. Hager,				5d. PROJECT NUMBER 4866	
				5e. TASK NUMBER LB	
				5f. WORK UNIT NUMBER 11	
7. PERFORMING ORGANIZATION NAME(S) AND ADDRESS(ES) AFRL/DELC 3550 Aberdeen Ave SE Kirtland AFB, NM 87117-5776				8. PERFORMING ORGANIZATION REPORT NUMBER *University of New Mexico Dept. of Mechanical Engineering Schooles Hall, Room 102 Albuquerque, NM 87117-0001	
9. SPONSORING / MONITORING AGENCY NAME(S) AND ADDRESS(ES) Air Force Research Laboratory 3550 Aberdeen Ave SE Kirtland AFB, NM 87117-5776				10. SPONSOR/MONITOR'S ACRONYM(S) AFRL/DELC	
				11. SPONSOR/MONITOR'S REPORT NUMBER(S) AFRL-DE-PS-TP-2007-1004	
12. DISTRIBUTION / AVAILABILITY STATEMENT Approved for Public Release; Distribution is Unlimited					
13. SUPPLEMENTARY NOTES Published in 36 th AIAA Plasmadynamics and Lasers Conference, June 2006, San Francisco, CA, by American Institute of Aeronautics and Astronautics (AIAA). This material is declared a work of the U.S. Government and is not subject to copyright protection in the United States.					
14. ABSTRACT Planar Laser-Induced Fluorescence (PLIF) was used to visualize the flow of a supersonic nozzle with a single supersonic injector. The nozzle simulates Chemical Oxygen Iodine Laser (COIL) flow conditions with non-reacting, cold flows, where the injected flow is seeded with iodine. A laser sheet near 565nm excites the iodine, and the fluorescence is imaged with a gated, CCD camera. Streamwise and semi-spanwise (oblique-view) images were taken, where the presence of injected flow is highlighted. With these images, the flow structures are identifiable and the mixing quality between the primary and injected flow can be quantitatively measured. Histograms of image ensembles were taken at varying downstream locations to quantify the mixing quality of the flow.					
15. SUBJECT TERMS Supersonic, PLIF, COIL, injector, iodine, mixedness					
16. SECURITY CLASSIFICATION OF:			17. LIMITATION OF ABSTRACT SAR	18. NUMBER OF PAGES 9	19a. NAME OF RESPONSIBLE PERSON Slav Peytchev
a. REPORT Unclassified	b. ABSTRACT Unclassified	c. THIS PAGE Unclassified			19b. TELEPHONE NUMBER (include area code)

CLEARED
FOR PUBLIC RELEASE
AFRLIDE 0-79
5 MAY 86

PLIF Visualization and Quantitative Mixing Measurements of a Supersonic Injection Nozzle

Carrie A. Noren¹

*Department of Mechanical Engineering, University of New Mexico, Albuquerque, NM, 87131
Air Force Research Laboratory, Directed Energy Directorate, Kirtland AFB, NM, 87117*

C. Randall Truman² and Peter V. Vorobieff³

Department of Mechanical Engineering, University of New Mexico, Albuquerque, NM, 87131

Timothy J. Madden⁴

Air Force Research Laboratory, Directed Energy Directorate, Kirtland AFB, NM, 87117

and

Gordon D. Hager⁵

Air Force Institute of Technology, Wright Patterson AFB, OH, 45433

Planar Laser-Induced Fluorescence (PLIF) was used to visualize the flow of a supersonic nozzle with a single supersonic injector. The nozzle simulates Chemical Oxygen Iodine Laser (COIL) flow conditions with non-reacting, cold flows, where the injected flow is seeded with iodine. A laser sheet near 565nm excites the iodine, and the fluorescence is imaged with a gated, CCD camera. Streamwise and semi-spanwise (oblique-view) images were taken, where the presence of injected flow is highlighted. With these images, the flow structures are identifiable and the mixing quality between the primary and injected flow can be quantitatively measured. Histograms of image ensembles were taken at varying downstream locations. A mixing parameter, defined from the histograms, is used to measure the mixing quality with downstream distance.

I. Introduction

HISTORICALLY, Chemical Oxygen Iodine Lasers (COIL) employ supersonic nozzles in which iodine and carrier helium are injected into a mixture of helium and singlet delta oxygen, $O_2(^1\Delta)$, upstream of the nozzle throat, in the subsonic region. Designs in which iodine is injected in the supersonic region of the nozzle have the potential to provide improved performance. Injecting the iodine and carrier helium downstream of the nozzle throat decouples this flow from the Singlet Oxygen Generator (SOG), allowing changes to be made to the injected mass flow without affecting the pressure upstream in the flow from the SOG. When injected into the subsonic region, the iodine and carrier helium are approximately 17-20% of the SOG molar flow. By injecting the iodine and carrier helium into the supersonic region, the pressure decreases, which increases the velocity and decreases the partial pressure of $O_2(^1\Delta)$. A lower partial pressure and increased velocity decreases the rate of $O_2(^1\Delta)$ loss and a greater velocity decreases the time it takes to transport $O_2(^1\Delta)$ downstream of the throat, enabling more lasing at the exit of the nozzle. Nozzle designs with supersonic injection of iodine were studied by Nikolaev et al., Zagidullin et al., Barmashenko et al., and Madden et al.^{1,2,3,4}

The fluid mechanics of COIL nozzles have been studied numerically and experimentally. Numerical studies have been performed on chemical lasers with iodine injection in the subsonic region of the nozzle by Madden and Miller,

¹Graduate Research Student, AIAA Student Member

²Professor of Mechanical Engineering, AIAA Associate Fellow

³Assistant Professor of Mechanical Engineering

⁴Research Scientist, AIAA Senior Member

⁵Senior Research Scientist

AFRLIDE 06-175

Miller et al., Miller and Shang, Madden and Solomon, and Masuda et al.^{5,6,7,8,9} Madden and Miller numerically simulated iodine injection in the supersonic region.⁵ This aids in the understanding of the mixing phenomena in the fluid-dynamic flowfields. Planar Laser-Induced Fluorescence (PLIF), a non-intrusive method to image the flowfield, has been used to study the fluid mechanics of a COIL nozzle with iodine injection in the subsonic region by Rapagnani and Davis and Muruganandam et al.^{10,11}

Gruber et al. and Lee et al. experimentally studied transverse jets in supersonic crossflow cases.^{12,13} Although the gases used do not simulate COIL, they give relationships between the momentum of the jets and crossflow. This work aids in the understanding of injection penetration into a supersonic region and the factors that affect penetration distance and mixedness of the two flows.

Previously, Noren et al. performed PLIF experiments on a supersonic nozzle with supersonic iodine injection in the supersonic region of the nozzle. The nozzle was designed with applications to COIL chemistry, but did not have sufficient mixing between the secondary and primary flows.¹⁴ That study precedes the current experiments, where PLIF results will be used to design a nozzle with ample mixing between the primary and secondary flows.

In this study, the flowfield of a supersonic nozzle with a single supersonic injector was imaged with PLIF. The nozzle studied has mass flow characteristics applicable to COIL. With the iodine fluorescence imaged, the quality of mixing can be quantified with histograms. A histogram of an unmixed flow of two species will have multiple modes. There will be one peak at zero intensity (the primary flow), another peak at a high intensity (the fluorescing injected flow), and a possible third low-intensity peak representing the mixed flow. As the flow becomes mixed, the second and third peaks will trend closer to the first peak. This is because the injected species mixes with the primary species, diluting the seeded iodine, causing the fluorescence intensity to decrease.

II. Materials and Methods

A. PLIF Diagnostics

The PLIF system consists of a Neodymium: Yttrium-Aluminum-Garnet (Nd:YAG) laser, tunable dye laser, laser-sheet-forming optics, and a CCD camera. The Nd:YAG laser, at the second harmonic (532 nm), pumps the tunable dye laser. It has a 10-Hertz pulse rate and an 8- to 10-second pulse width. The output of the YAG laser is turned by two dichroic mirrors (425-675 nm) into the dye laser. The tunable dye laser, with Rhodamine 6G as the dye, has a 559 to 576 nm range with a peak at 566 nm. Maximum iodine fluorescence occurs at approximately 565 nm, which makes Rhodamine 6G ideal for this application. The pulse width of the dye laser is ~30 ns. The beam from the dye laser is turned, using a BK7 prism, into a series of three lenses to collimate and expand the beam into a rectangular sheet with minimal thickness (~600 μm). The dye laser is then used to excite the injected iodine molecules to stimulate fluorescence. This fluorescence is imaged with a gated CCD camera.

Once the dye laser beam is collimated and expanded, it is directed into the nozzle, either through the nozzle's Lexan window or through a calcium-fluoride window at the back end of the nozzle. The laser excites the iodine in the injected flow to stimulate fluorescence. This fluorescence is imaged with an intensified, gated CCD camera. The camera has 512 x 512 pixels and is gated at 20 ns. It is able to capture images at a rate of 10 Hz. To collect streamwise images, the laser sheet is aimed up the back-end of the nozzle (against the primary flow) and the camera is positioned perpendicular to the laser sheet and Lexan windows. For the oblique-view images, the laser sheet passes through the Lexan windows at a 45° angle. As in the streamwise images, the camera is aimed perpendicular to the laser sheet. Figure 1 is a schematic of the nozzle block, camera, and laser sheet positioned in the oblique view. With the oblique-view set up, the power of the laser is reduced to 25 mJ so as to not burn the Lexan.

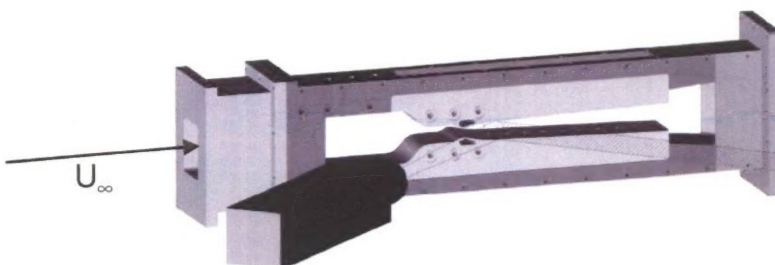


Figure 1. Schematic of the nozzle, with the flow from left to right. The laser sheet passes through the Lexan window, angled 45° to the primary flow. The camera, as shown, acquires images perpendicular to the laser sheet, which gives the oblique-view images.

B. Nozzle Hardware

The nozzle test stand includes the nozzle frame, a flow-straightener upstream of the nozzle, and two nozzle contour inserts. The nozzle contour inserts are removable so that injectors may be added for future testing. The nozzle is designed for a primary flow of Mach 2.2. The throat height is 1 cm, and the distance from the throat to the exit of the nozzle is 22.5 cm. The single injector is located on the bottom nozzle contour insert, 0.25 cm downstream of the throat. It is angled 45° to the primary flow. The exit to throat area ratio for the injector is 4, giving a design Mach number of 3.4. Figure 2 displays the geometry of the single injector.

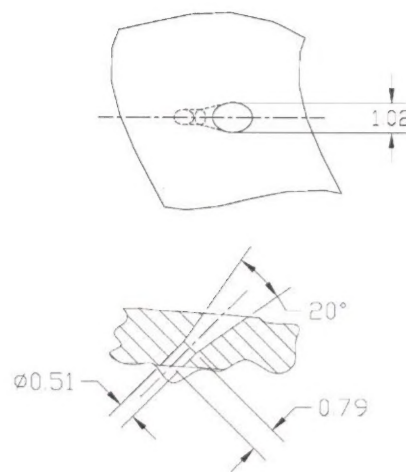


Figure 2. Schematics of the injector geometry, units given in millimeters.

C. Gas Flows

The primary flow consists of helium at 505 mmol/s and oxygen at 125 mmol/s. A COIL nozzle would have a series of rows of injectors to produce a well-mixed medium of secondary and primary flow. To simulate COIL chemistry, the secondary flow would have 125 mmol/s of helium and about 1 mmol/s of iodine. In this experiment, however, only one of the injectors is present, which contributes approximately 1% of the secondary flow. The secondary flow system is set up to deliver the 125 mmol/s of helium and 1 mmol/s of iodine. To easily and accurately deliver only 1% of this flow to the injector, the secondary gas flow is fractionated with an orifice, where 99% of the flow bypasses the injector and 1% is sent to the injector. The iodine molar flow rate is measured in the flow before fractionation. The absorbance measurement of an Argon-Ion laser beam (488 nm) through the flow of helium and iodine is used to determine the concentration of iodine in the flow. From the iodine concentration, helium flow rate, pressure, and temperature in the flow, the molar flow rate can be deduced. Davis gives a complete review of this procedure.¹⁵

III. Results

The nozzle was tested with and without a single injector. Pressure measurements were taken when the nozzle without the single injector (blank nozzle contour inserts) was on the test stand. The pressure measurements were used to compute the Mach number in the nozzle. Streamwise and oblique-view PLIF images were acquired when the nozzle with the single injector was on the test stand.

A. Mach Number Measurements

To verify the design, the nozzle without the single injector was placed on the test stand so that pressure measurements could be made. One of the smooth Lexan walls was replaced with a Lexan wall that had fittings at 2.5-cm increments. A Pitot tube could be inserted in these fittings. Because the flow is supersonic, the stagnation pressures upstream and downstream of the shock wave formed by the Pitot tube were used to calculate the Mach number in the flow. The isentropic relationship for pressure and Mach number and the relationship for Mach numbers up- and downstream of a normal shock were used to determine the Mach number from the ratio of stagnation pressures. The relationship between the Mach number upstream of the normal shock wave, M_1 , and the ratio of stagnation pressures, where P_{01} is the stagnation pressure upstream of the normal shock and P_{02} is the stagnation pressure downstream of the normal shock, is

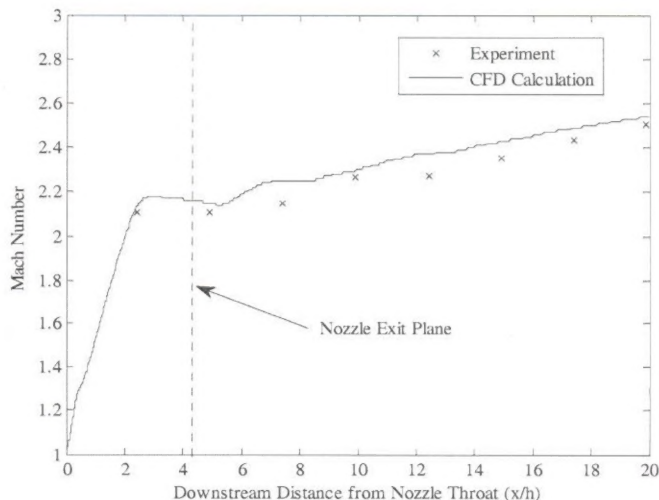


Figure 3. Mach number versus downstream distance as measured with stagnation pressures and as calculated with 3-D CFD.

$$\frac{P_{02}}{P_{01}} = \left(\frac{\frac{\gamma+1}{2} M_1^2}{1 + \frac{\gamma-1}{2} M_1^2} \right)^{\frac{\gamma}{\gamma-1}} \left(\frac{2\gamma}{\gamma+1} M_1^2 - \frac{\gamma-1}{\gamma+1} \right)^{\frac{1}{1-\gamma}}. \text{ The ratio of specific heats for the gas is represented by } \gamma.^{16}$$

The stagnation pressure upstream of the normal shock was measured in the plenum of the nozzle, whereas the stagnation pressure downstream of the normal shock wave was measured by the Pitot tube. The Pitot tube was placed along the centerline of the nozzle. The Mach number distribution, as determined from the measured stagnation pressures, is displayed in Fig. 3. The downstream distance is normalized by the nozzle throat height, h . At the nozzle exit plane, the Mach number is close to the design number of 2.2. Along with the experimental results, Fig. 3 displays the Mach number from a computational fluid dynamics (CFD) calculation for this nozzle. Additional CFD results will be presented in a subsequent paper.

B. PLIF Imaging

Streamwise and oblique-view images were collected in ensembles of 100 at various downstream locations. In these images, the presence of the injected flow is highlighted with the iodine fluorescence. Three oblique-view ensemble-averaged images are displayed in Fig. 4. In each image, the counter-rotating vortex pair is visible. The structure height grows with downstream distance, which indicates jet penetration with downstream distance.

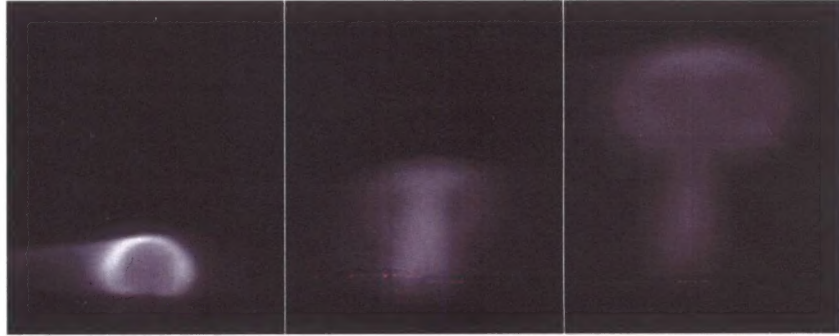


Figure 4. Ensemble-averaged images of the injector jet in the oblique view at a) $x/h = 0.28$, b) $x/h = 0.58$, and c) $x/h = 0.98$. The image width is 224 pixels and the image height is 270 pixels, where each pixel is 0.05mm.

Figure 5 displays ensemble-averaged streamwise images. These images were acquired along the centerline of the jet. Each ensemble consists of 100 images. Figure 5 (a) is taken with the nozzle throat at the left-hand-side of the image. The origin of each consecutive image is located at the right-hand-side of the previous image; there is no overlap between the images. The portion of the jet that is brightest is the less-mixed injector flow, the counter-rotating vortex pair (CRVP). The flow below the bright portion of the jet is a well-mixed flow of primary and secondary gases, and the dark portions of the images represent the unmixed freestream.

C. Streamwise Image Analysis

To quantify the mixing behavior of the secondary and primary flows, histograms of the fluorescence intensity in the streamwise images were created. Histograms display the probability density of the intensity. For each image, the intensity was normalized by the maximum intensity of the streamwise image at the injector exit (Fig. 5 (a)), which is the maximum intensity for all the streamwise images. Figure 6 displays a histogram including all eight streamwise images. Image (a) and (b) have a large peak at zero intensity (the unmixed freestream) and another peak at a higher intensity (the CRVP). The histograms for (a) and (b) do not show a peak at low intensity which would indicate a well-

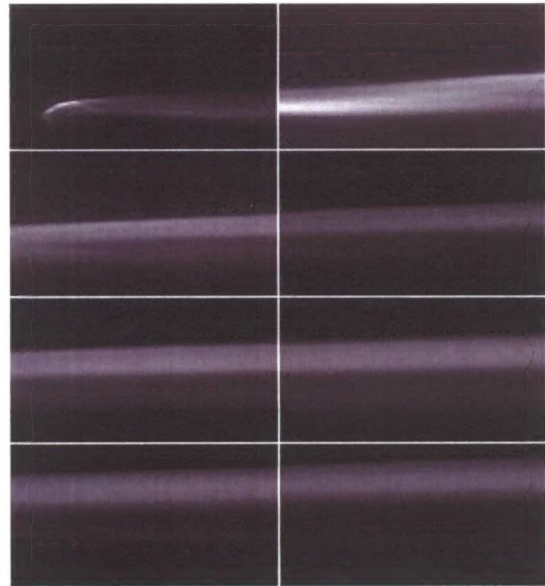


Figure 5. Ensemble-averaged images of the injector jet in the streamwise view at progressive downstream positions from the nozzle throat.

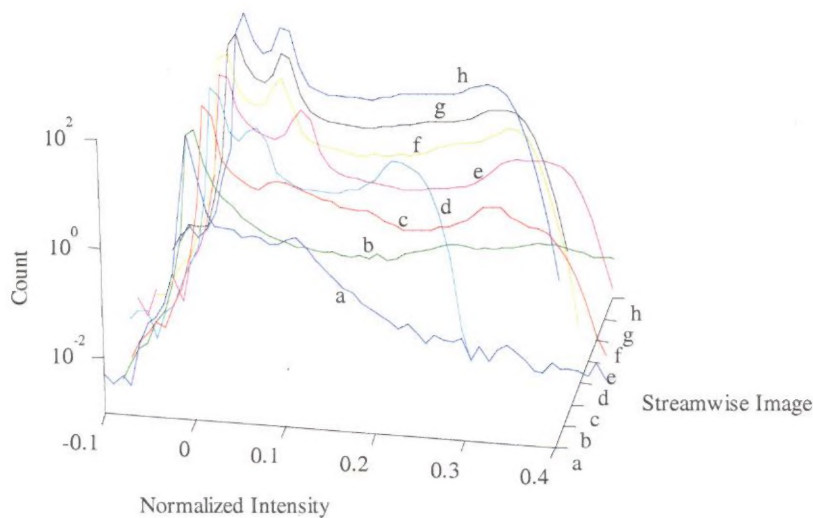


Figure 6. Histograms of the ensemble-averaged images displayed in Fig. 5 (a)-(h). Intensity is normalized by the maximum intensity in Fig. 5 (a).

overlapping segments as shown in Fig. 7. Each segment has a pixel width of 128 and a pixel height of 282. The horizontal overlap between adjacent segments is 64 pixels. Histograms were created for each segment and mapped together for comparison. Figure 8 displays the histograms from Fig. 5 (c). Each histogram includes three peaks and the second and third peaks decrease in intensity as did the histograms (c) through (h) in Fig. 6. The histograms for Fig. 5 (h) are shown in Fig. 9. Similar to the histograms in Fig. 8, there are three peaks. The peaks, however, do not decrease in intensity value with downstream distance. This infers that the flow is not significantly developing at this downstream distance, like it is farther upstream in Fig. 5 (c).

mixed flow between the primary and secondary flows. The histograms for images (c) through (h) each have three peaks, including a large peak at zero intensity representing the freestream, a peak at low intensity indicating a well-mixed flow, and a peak at high intensity representing the less-mixed injected flow. As the downstream distance increases, the intensity values characterizing the second and the third peak move toward the value indicative of the freestream (main) flow, which suggests that the flow is getting more mixed and that the main flow gases are advected into the CRVP.

Each streamwise image was divided into seven different

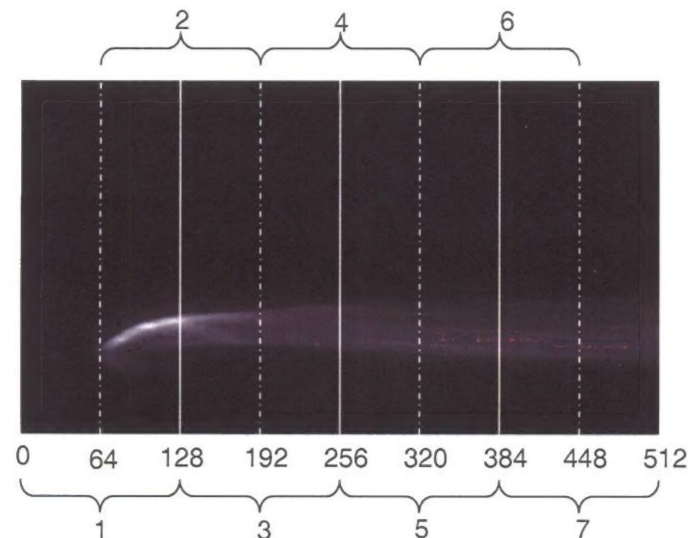


Figure 7. A schematic displaying how each streamwise image was divided to create seven histograms for each image. The numbers by the brackets refer to the image section number, while the numbers directly under the image refer to the image pixel.

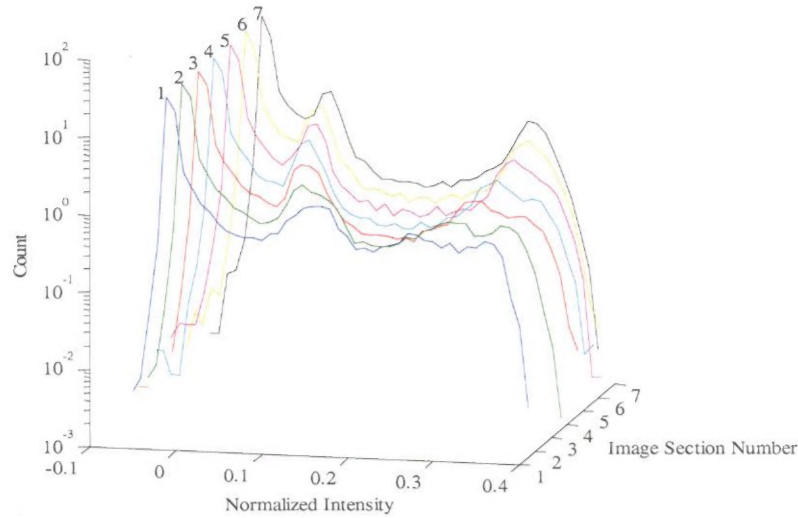


Figure 8. Histograms of seven overlapping sections from Fig. 5 (c). Intensity is normalized by the maximum intensity in Fig. 5 (a).

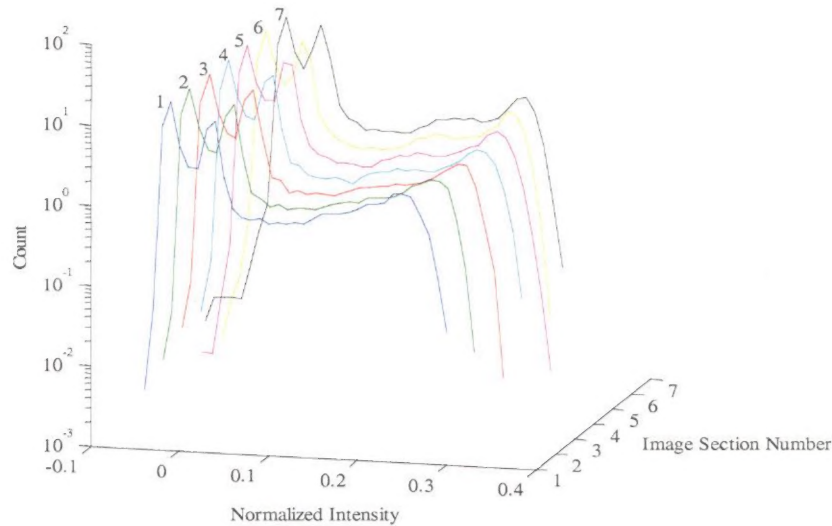


Figure 9. Histograms of seven overlapping sections from Fig. 5 (h). Intensity is normalized by the maximum intensity in Fig. 5 (a).

IV. Discussion

In this study, a PLIF diagnostic was used to image the injected flow in the supersonic region of a supersonic nozzle. A histogram analysis was performed on ensemble averages of streamwise images to quantify the mixing between the primary and secondary flows. The histograms revealed three regions of the flow: 1) the zero-intensity primary flow, 2) the high-intensity secondary flow structure, and 3) the intermediate-intensity well-mixed flow with recirculation. From the histograms of the streamwise images, the flow becomes better-mixed with downstream distance. Also, the flow becomes fully developed before the exit of the nozzle, where mixing quality does not increase drastically with downstream distance.

Additional injectors will be added to this nozzle to produce a well-mixed medium of primary and secondary flows. With each additional injector, PLIF will be used to analyze the flow for desired penetration and mixing quality. The next injector being considered is a small injector directly downstream of the current single injector to stimulate flow turbulence.

Acknowledgments

C. A. Noren thanks Drs. Steven Davis and Shawn Wehe from Physical Sciences, Inc. for designing and delivering the PLIF diagnostic equipment (which includes the lasers, camera, and sheet-forming optics). C. A. Noren also thanks Greg Johnson, Norma McMackin, and Lt. Slav Peytchev for their technical help in the laboratory and Rick Dow for his mechanical design assistance.

References

- ¹Nikolaev, V. D., Zagidullin, M. V., Svistun, M. I., Anderson, B. T., Tate, R. F., and Hager, G. D., "Results of Small-Signal Gain Measurements on a Supersonic Chemical Oxygen Iodine Laser with an Advanced Nozzle Bank," *IEEE Journal of Quantum Electronics*, Vol. 38, 2002, pp. 421-428.
- ²Zagidullin, M. V., Nikolaev, V. D., and Hager, G. D., "High Gain, High Pressure, Highly Efficient COIL," *High-Power Laser Ablation V, Proceedings of the SPIE*, Paper 5448-169, Vol. 5448, C. R. Phipps, ed., 2004, pp. 1139-1149.
- ³Barmashenko, B., Rybalkin, V., Katz, A., and Rosenwalks, S., "Parametric study of the Ben-Gurion University Efficient Supersonic Chemical Oxygen-Iodine Laser," *High-Power Laser Ablation V, Proceedings of the SPIE*, Vol. 5448, No. 1, C. R. Phipps, ed., 2004, pp. 282-293.
- ⁴Madden, T. J., Hager, G. D., Lampson, A. I., and Crowell, P. G., "An Investigation of Supersonic Mixing Mechanisms for the Chemical Oxygen-Iodine Laser (COIL)," *30th Plasmadynamics and Lasers Conference*, AIAA 99-3429, Jun. 1999.
- ⁵Madden, T. J. and Miller, J. H., "Simulation of Flow Unsteadiness in Chemical Flowfields," AIAA Paper 2004-0805.
- ⁶Miller JH, Shang JS, Tomaro RF, Strang WZ (2001) Computation of compressible flows through a chemical laser device with crossflow injection. *J Propul Power* 17(4): 836-844
- ⁷Miller, J. H. and Shang, J. S., "Parallel Computation of Chemical Oxygen/Iodine Laser Flowfields" *32nd Plasmadynamics and Lasers Conference*, AIAA 2001-2869, Jun. 2001.
- ⁸Madden, T. J. and Solomon, W. C., "A Detailed Comparison of a Computational Fluid Dynamic Simulation and a Laboratory Experiment for a COIL Laser," *28th Plasmadynamics and Lasers Conference*, AIAA 97-2387, June 1997.
- ⁹Masuda, W., Hishida, M., Hirooka, S., Azami, N., and Yamada, H., "Three-Dimensional Mixing/Reacting Zone Structure in a Supersonic Flow Chemical Oxygen-Iodine Laser," *JSME International Journal, Series B—Fluids and Thermal Engineering*, Vol. 40, No. 2, 1997, pp. 209-215.
- ¹⁰Rapagnani, N. L. and Davis, S. J., "Laser-Induced I₂ Fluorescence Measurements in a Chemical Laser Flowfield," *AIAA Journal*, Vol. 17, No. 12, 1979, pp. 1402-1404.
- ¹¹Muruganandam, R. M., Lakshmi, S., Ramesh, A. A., Viswamurthy, S. R., Sujith, R. I., and Sivaram, B. M., "Mixing of Transversely Injected Jets into a Crossflow Under Low-Density Conditions," *AIAA Journal*, Vol. 40, No. 7, Jul. 2002, pp. 1388-1394.
- ¹²Gruber, M. R., Nejad, A. S., Chen, T. H., and Dutton, J. C., "Transverse Injection from Circular and Elliptic Nozzles into a Supersonic Crossflow," *Journal of Propulsion and Power*, Vol. 16, No. 3, May-June, 2000, pp. 449-457.
- ¹³Lee, M. P., McMillin, B. K., Palmer, J. L., and Hanson, R. K., "Planar Fluorescence Imaging of a Transverse Jet in a Supersonic Crossflow," *Journal of Propulsion and Power*, Vol. 8, No. 4, Jul.-Aug. 1992, pp. 729-735.
- ¹⁴Noren, C. A., Rothschof, G., Perschbacher, T., Madden, T. J., Hager, G. D., Truman, C. R., Vorobieff, P. V., "PLIF Flow Visualization of a Supersonic Injection COIL Nozzle," *36th Plasmadynamics and Lasers Conference*, AIAA Paper 2005-5388, Jun. 2005.
- ¹⁵Davis, S. J., U.S. Patent 4,467,474, "Halogen Mass Flow Rate Detection System," 21 Aug. 1984.
- ¹⁶Lifshitz, E. M. and Landau, L. D., *Fluid Mechanics, Second Edition (Course of Theoretical Physics, Volume 6)*, Butterworth-Heinemann, Jordon Hill, Oxford, 1987, p 319.